

Comparison of Early Postoperative Stress Distribution around Short and Tapered Wedge Stems in Femurs with Different Femoral Marrow Cavity Geometries Using Finite Element Analysis

Tsuguaki Hosoyama, MD, Nobuhiro Kaku, MD, Jonas A. Pramudita, PhD Eng*, Yutaro Shibuta, MD

Department of Orthopaedic Surgery, Faculty of Medicine, Oita University, Yufu,

**Department of Mechanical Engineering, College of Engineering, Nihon University, Koriyama, Japan*

Background: In total hip arthroplasty (THA), the ideal stem length remains uncertain; different stem lengths are used in different cases or institutions. We aimed to compare the stress distributions of cementless tapered wedges and short stems in femurs with different femoral marrow geometries and determine the appropriate fit.

Methods: Finite element models were created and analyzed using HyperMesh and LS-DYNA R11.1, respectively. The 3-dimensional shape data of the femurs were extracted from computed tomography images using the RETOMO software. Femurs were divided into 3 groups based on the Dorr classification. The computer-aided design data of cementless tapered wedge-type and short stems were used to select the appropriate size. In the finite element analysis, the loading condition of the femur was assumed to be walking. Volumes of interest (VOIs) were placed within the femur model at the internal and external contact points of the stem based on Gruen zones. The average stresses and strain energy density (SED) of the elements included in each VOI were obtained from the preoperative and postoperative models.

Results: The von Mises stress and SED distributions of the cementless tapered wedge and short stems were similar in their respective Dorr classifications. In both stems, the von Mises stress and SED after THA were lower than before THA. The von Mises stress and SED of the cementless tapered wedge stem were higher than those of short stems. Cementless tapered wedge-type stems tended to have lower rates of change than short stems; however, Dorr C exhibited the opposite trend. In the Dorr classification comparison, the von Mises stress and SED were greater for both stems in the order of Dorr C > Dorr B > Dorr A, from Zone 2 to Zone 6.

Conclusions: In Dorr A and B, the short stem exhibited a natural stress distribution closer to the preoperative femur than the tapered wedge stem; however, in Dorr C, the short stem may have a greater effect on stress distribution, suggesting that it may cause greater effects, such as fracture in the early postoperative period, than other Dorr types.

Keywords: Femur, Hip prosthesis, Finite element analysis, Stress, Classification

Received November 9, 2023; Revised May 24, 2024;

Accepted May 24, 2024

Correspondence to: Nobuhiro Kaku, MD

Department of Orthopaedic Surgery, Faculty of Medicine, Oita University,
1-1 Idaigaoka Hazama-machi, Yufu, Oita 879-5593, Japan

Tel: +81-97-586-5872, Fax: +81-97-586-6647

E-mail: nobuhiro@oita-u.ac.jp

In total hip arthroplasty (THA), the length of the femoral component affects the stem alignment at the time of placement, early postoperative fixation, and fracture;^{1,2)} however, the ideal stem length remains unknown, and in practice, different stem lengths are used in different cases or institutions.²⁾

The cementless tapered wedge stem can be crimp-fixed to the proximal femur owing to its shape, and de-

spite being smaller in volume than the conventional fit and fill-type cylindrical stem, it provides initial stability owing to appropriate mechanical loading on the femur.³⁾ Comparative bone preservation has been achieved using cementless tapered wedge stems, and the risk of proximal stress shielding and periprosthetic fractures has also been reduced.⁴⁾ In addition, excellent long-term survival results have been achieved; however, residual proximal stress shielding and femoral pain have been observed.⁵⁾

Similar to the number of initial THAs, the number of revision THAs is also increasing,⁶⁾ and the possibility of future revision THAs should be considered during the initial THA, especially in young and active patients. Consequently, short stems that are less invasive to the femoral bone marrow cavity and more bone-sparing have been developed.⁷⁾ Depending on the model, short stems are designed to have a better fit in the proximal femur than the tapered-wedge type to reduce stress shielding and achieve a load distribution in the proximal femur that closely mimics the physiological distribution. Although short- and mid-term results are excellent,⁸⁾ short-stem fixation has been associated with a lower initial fixation force owing to the small contact area and relatively high risk of postoperative fracture.⁹⁾

Dorr classified femoral geometry into 3 categories, and the distribution of mechanical load in the femur after THA is also influenced by the patient's femoral marrow cavity geometry. A mismatch between the size of the cementless tapered wedge stem and the shape of the proximal femoral medullary cavity is associated with poor prognosis.¹⁰⁾ Short stems are no exception, especially Dorr type C with a wide femoral medullary cavity, which, together with poor bone quality, makes it difficult to obtain sufficient strength for initial stem fixation,¹¹⁾ resulting in a high incidence of fractures¹²⁾ and stress shielding after biological fixation.¹³⁾

Literature verifying whether a short stem length design reproduces the preoperative physiological stress distribution in the proximal femur is lacking.¹⁴⁾ In addition, to determine the appropriate adaptation of the stem

model, analyzing the stress distribution in the surrounding bone after the placement of each stem for different femoral marrow cavity geometries is necessary. The existing short and tapered wedge stems should be used to obtain more realistic results. The tapered wedge-type Profemur TL (MicroPort Orthopedics) and the short stem-type Profemur Preserve (MicroPort Orthopedics) are artificial hip joint stems manufactured by the same company, and both have a diaphyseal end fixation. To our knowledge, no study has used finite element analysis to directly compare an existing tapered wedge stem with a short stem for different femoral marrow cavity geometries. The objectives of this study were to (1) compare the stress distribution in the preoperative femur with the Dorr classification of marrow cavity geometry with that of the tapered wedge and short stem in the early postoperative period and (2) compare the stress distribution in the surrounding femur of the short stem and tapered wedge stem for each medullary cavity geometry.

METHODS

This study was conducted in accordance with the principles of the Declaration of Helsinki and approved by the Ethics Committee of Oita university (IRB No. 1650, approval date: October 18, 2019). Written informed consent was obtained from the clinical cases and femur patients used for modeling.

Analytical Model

Finite element models were created, and finite element analyses were performed using HyperMesh (Altair Engineering Inc.) and LS-DYNA R11.1 (Ansys Inc.), respectively. Femur 3-dimensional (3D) shape data were obtained by extracting only the femur from the computed tomography (CT) images and stacking them using the 3D modeling software RETOMO (BETA CAE Systems International). Of the 26 cases and 29 joints that underwent THA for hip osteoarthritis due to acetabular dysplasia using MicroPort's Preserve stem between August 2019 and

Table 1. Clinical Characteristics of Each Case

Case	Age (yr)	Height (cm)	Weight (kg)	BMI (kg/m ²)	BMD (g/cm ²)	Dorr classification	CFI
F1	59	159	48.0	19.0	0.802	A	5.82
F2	71	147	53.4	25.0	1.249	B	3.55
F3	62	148	65.0	29.7	0.650	C	2.99

BMI: body mass index, BMD: bone mineral density, CFI: canal flair index.

February 2023, 28 joints in 25 female patients, for whom postoperative CT imaging was available and consent forms were obtained, were included. The canal flair index (CFI) of each femur was measured and divided into 3 Dorr groups (Dorr A: 7 cases, B: 17 cases, and C: 1 case), from which 1 case was randomly selected. Patients' age, height, weight, body mass index, and bone mineral density of the lumbar spine, along with CFI, are presented in Table 1. The post-THA radiographs of patients are shown in Fig. 1. Based on the CFI, each femur was designated as Dorr A, B, or C. The actual stem sizes used and their design drawings are shown in Fig. 2.

The coordinate system of the femur was Bergmann's coordinate system.¹⁵⁾ The z-axis is the stem axis, the Y-axis is a straight line drawn from the back to the front passing through the origin, and the x-axis is a straight line passing through the origin and orthogonal to the Y-axis and Z-

axis. The femoral neck was sectioned along the stem shape using a 3D finite element model of the femur, and the stem was placed. The computer-aided design (CAD) data of MicroPort's tapered-wedge type Profemur TL for the cementless stem and Preserve for the short stem were used. The appropriate size was selected using the ZedHip (Lexi Co., Ltd., Tokyo, Japan), tangent to the medial cortical bone line that outlines the medullary cavity. Finite element models of both stems were constructed based on the CAD data. In both model scenarios, the stems were installed at a stem height that did not cause any difference in leg length.

The stems were placed in the intermediate position, aligning the stem axis with the femoral bone axis and the stem neck axis with the femoral neck axis. The femur

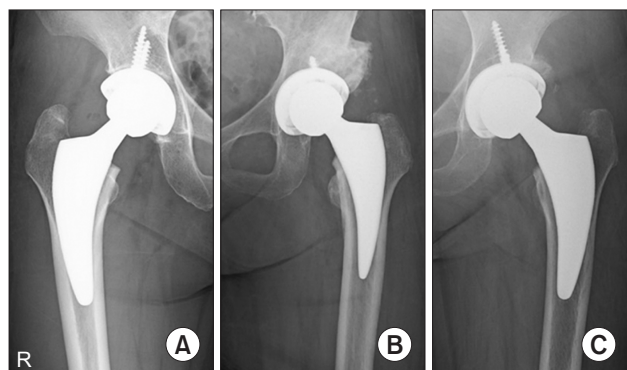
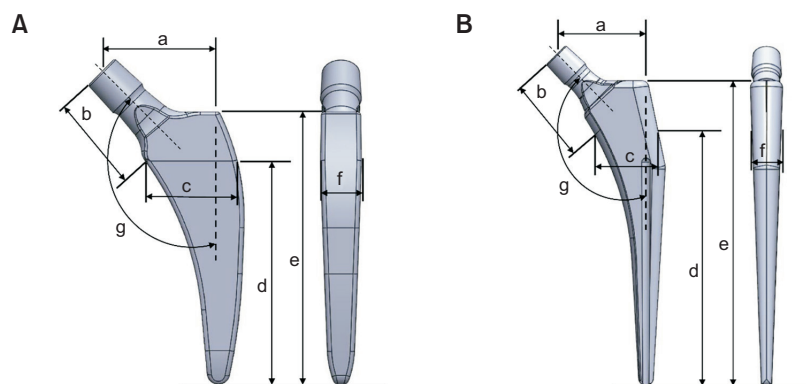


Fig. 1. Radiographs obtained after total hip arthroplasty. (A) Dorr A. (B) Dorr B. (C) Dorr C.

Table 2. Nodes and Elements of the Finite Element Model for Each Case

Case	Stem type	Node	Element
F1	Preoperative	55,699	257,516
	Short stem	58,176	268,095
	Tapered wedge stem	56,438	259,797
F2	Preoperative	44,179	200,731
	Short stem	44,512	199,599
	Tapered wedge stem	43,861	197,471
F3	Preoperative	47,191	210,782
	Short stem	44,855	197,861
	Tapered wedge stem	48,956	218,434



	Preserve stem size	a (mm)	b (mm)	c (mm)	d (mm)	e (mm)	f (mm)	g (°)	TL stem size	a (mm)	b (mm)	c (mm)	d (mm)	e (mm)	f (mm)	g (°)
F1	#6	46	33	32.5	81	97.5	13.7	127	#5	42	35	30	119	144	13	127
F2	#1	41	29	28.7	75	91.5	13.0	127	#3	38	30	29	114	135	13	127
F3	#5	46	33	31.7	78	94.5	13.6	127	#4	42	35	30	116	142	13	127

Fig. 2. Dimensions of the short stem and tapered wedge stem. (A) Profemur Preserve stem. (B) Profemur TL stem.²¹⁾

and stem models comprised 4-node tetrahedral elements with an element size of 2.0 mm; the number of elements and nodes for each model are presented in Table 2. In the finite element analysis, the load constraint condition of the femur was assumed to be walking (Fig. 3). The material properties of the finite element models and the loads acting on the femur and stem are listed in Tables 3 and 4, respectively.^{16,17)}

The distal femur was assumed to be fully constrained. For the femur model, the volumes of interest (VOIs) were placed at the internal and external contact points of the stem based on Gruen zones (Fig. 4).¹⁸⁾ The average values of the pre- and postoperative stress and strain energy densities (SEDs) of the elements included in each VOI were calculated. For the contact conditions between the stem and femur, the static friction coefficient and dynamic wear coefficient between the stem and sea surface bone and between the stem and cortical bone were set to 0.64 and 0.3, respectively.¹⁹⁾ The load was assumed to increase linearly and reach a maximum value at 0.2 seconds, and the calculations were performed using the implicit dynamic method.²⁰⁾ Mechanical parameters such as von Mises stress and SED were calculated.

RESULTS

The von Mises stress distribution and SED in the pre- and postoperative Dorr classifications are illustrated in Fig. 5. The patients were assumed to be in a walking condition with body weight at F1. For both Preserve and TL, the

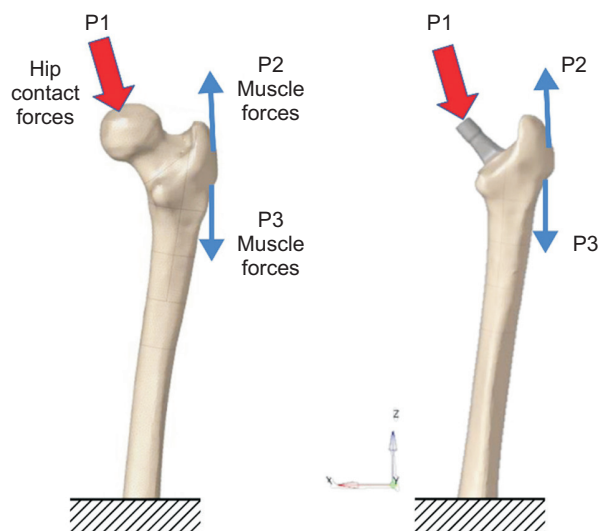


Fig. 3. Loads applied to the finite element model during walking. The distal femur was assumed to be fully constrained, and the loading conditions were those of walking.²¹⁾

von Mises stress and SED were highest in zone 4 or zone 5 and lowest in zone 1 or zone 7. All exhibited a mountain-shaped distribution with similar results. Stress distribution and SED were similar for each Dorr classification system. In both stems, the postoperative von Mises stress and SED were lower than the preoperative values ($p < 0.05$). The von Mises stress and SED of the TL were higher than those of the Preserve.

A comparison of the Dorr classifications is illustrated in Fig. 6. For both stems, the von Mises stress and SED were in the following order: Dorr C > Dorr B > Dorr A for zones 2 to 6 ($p < 0.05$). The rates of change in the von Mises stress and SED are listed in Tables 5 and 6, respectively. The rates of change in the von Mises stress and SED tended to be smaller in zone 4 or zone 5 and larger in zone 1 or zone 7. They also tended to be smaller in the Preserve than in the TL; however, Dorr C exhibited the opposite trend. Excluding the results of zone 1 for Dorr B in the Preserve, the rates of change in the von Mises stress and SED tended to be larger for both stems in the following order: Dorr A > Dorr B > Dorr C. The rates of change in the von Mises stress and SED for Dorr B in Preserve tended to be larger than that for Dorr A in Preserve; however, the opposite

Table 3. Material Properties (Linear Elastic Materials) Used in the Finite Element Simulations

	Density (g/cm ³)	Young's modulus (GPa)	Poisson's ratio
Cortical bone	1.8	17.5	0.3
Cancellous bone	0.8	10.0	0.3
Stem	4.4	113.0	0.3

Table 4. Load Acting on the Femur and Stem

Case		X (N)	Y (N)	Z (N)
F1	P1	254	-154	-1,079
	P2	305	71.5	380
	P3	-4.24	87.1	-437
F2	P1	-282	-171	-1,201
	P2	339	79.6	423
	P3	-4.71	96.9	-487
F3	P1	-344	-209	-1,461
	P2	413	96.9	515
	P3	-5.74	118	-59

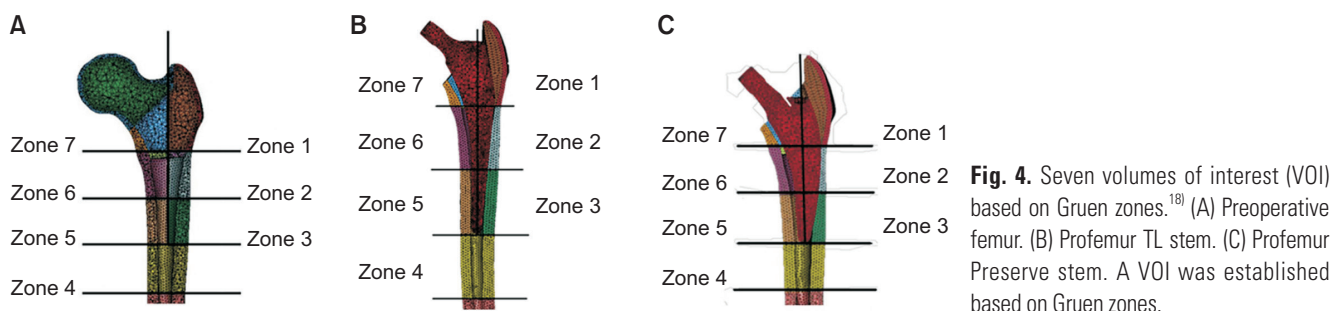


Fig. 4. Seven volumes of interest (VOI) based on Gruen zones.¹⁸⁾ (A) Preoperative femur. (B) Profemur TL stem. (C) Profemur Preserve stem. A VOI was established based on Gruen zones.

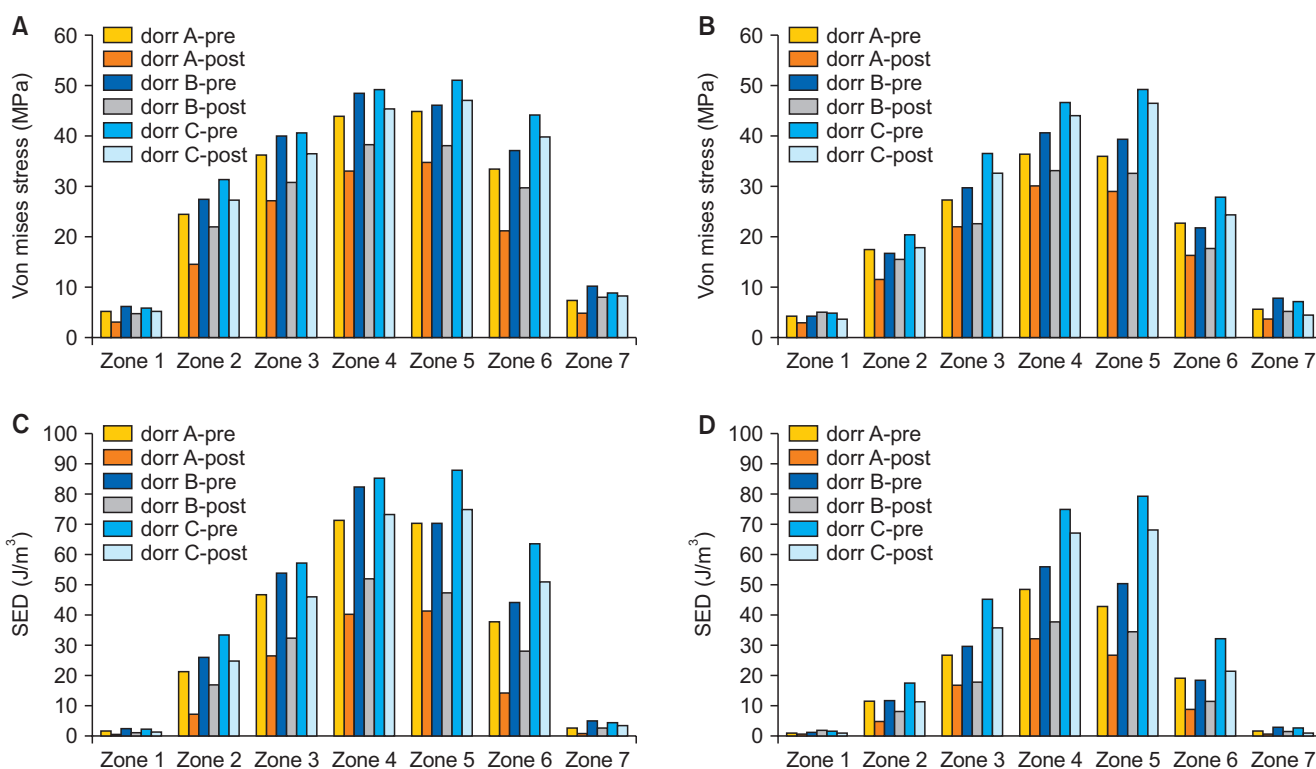


Fig. 5. Comparison of pre- and postoperative von Mises stress in TL and Preserve for each Dorr classification. (A, C) Profemur TL stem. (B, D) Profemur Preserve stem. The loads were analyzed using the weight of F1. In both stems, the postoperative von Mises stress was lower than the preoperative values. The von Mises stress in the TL was greater than that in Preserve. Comparing the Dorr classification, the von Mises stress was greater for both stems in the following order: Dorr C > Dorr B > Dorr A ($p < 0.05$). SED: strain energy density.

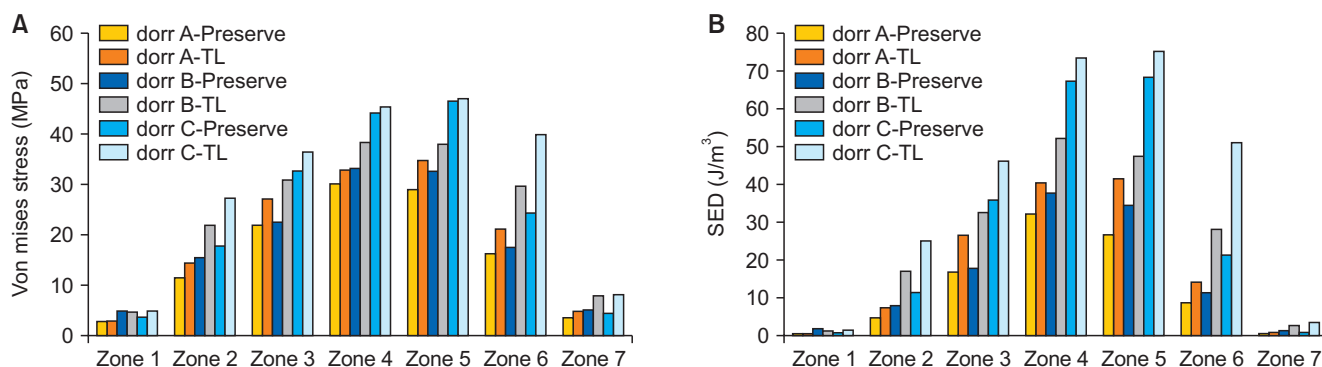


Fig. 6. Comparison of Preserve and TL for each Dorr classification. (A) von Mises stress. (B) Strain energy density (SED). Analysis was performed for F1 body weight, and the von Mises stress and SED of TL were greater than those of Preserve ($p < 0.05$).

Table 5. Rate of Change of von Mises Stress in Profemur TL and Profemur Preserve

VOI	Profemur TL			Profemur preserve		
	Dorr A	Dorr B	Dorr C	Dorr A	Dorr B	Dorr C
Zone 1	-41.80	-22.70	-13.70	-30.00	19.90	-21.80
Zone 2	-40.80	-20.70	-13.00	-34.30	-7.00	-12.60
Zone 3	-25.20	-22.80	-10.20	-20.00	-23.80	-10.40
Zone 4	-25.10	-20.90	-7.50	-17.10	-18.60	-5.50
Zone 5	-22.60	-17.80	-8.00	-19.30	-17.00	-5.50
Zone 6	-36.60	-19.90	-9.60	-28.50	-18.90	-12.50
Zone 7	-34.20	-21.50	-7.10	-36.00	-33.50	-38.30
Average	-32.30	-20.90	-9.90	-26.50	-14.10	-15.20

Values are presented as percentage (%).

VOI: volume of interest.

Table 6. Percentage Change in SED in Profemur TL and Profemur Preserve

VOI	Profemur TL			Profemur preserve		
	Dorr A	Dorr B	Dorr C	Dorr A	Dorr B	Dorr C
Zone 1	-72.90	-50.80	-37.70	-54.90	41.20	-46.40
Zone 2	-65.20	-38.40	-25.70	-58.80	-31.20	-35.10
Zone 3	-43.40	-40.00	-19.50	-37.00	-39.70	-21.10
Zone 4	-43.40	-36.80	-14.00	-33.60	-32.60	-10.30
Zone 5	-41.10	-32.70	-14.50	-37.60	-31.40	-13.90
Zone 6	-62.20	-36.30	-19.80	-54.60	-38.20	-33.50
Zone 7	-65.00	-45.50	-20.40	-65.30	-49.10	-65.20
Average	-56.20	-40.10	-21.70	-48.80	-25.80	-32.20

Values are presented as percentage (%).

SED: strain energy density, VOI: volume of interest.

Table 7. Stem Occupancy of Profemur TL and Profemur Preserve to Femur

	Stem volume (mm ³)		Femur volume (zones 1, 2, 3, 5, 6, 7) (mm ³)		Volume fraction	
	Preserve	TL	Preserve	TL	Preserve	TL
Dorr A	20,393	21,461	69,975	86,878	0.29	0.25
Dorr B	15,251	17,704	52,935	64,759	0.29	0.27
Dorr C	20,161	22,715	53,314	67,586	0.38	0.34

was observed for Dorr C. Table 7 presents the occupancy of both stems in relation to the femur, with Preserve having a larger volume fraction than TL. The occupancy of

Dorr C was 0.38 larger than that of Dorr A and Dorr B.

DISCUSSION

Short stems are primarily designed to achieve a better fit in the proximal femur than the tapered wedge-type and to promote a more natural load distribution in the proximal femur. However, the extent to which short stems can truly reproduce the physiological stress distribution in the preoperative proximal femur remains uncertain. The load distribution around the stem depends on the geometry of the femoral marrow cavity. Therefore, in this study, we conducted a direct comparison between the existing tapered wedge stem and the short stem using finite element models. For both Preserve and TL, the von Mises stress and SED were the highest in Zones 4 or 5 and the lowest in zones 1 or 7. The results were similar, exhibiting a mountain-shaped distribution in both cases. Stress distribution and SED were similar for each Dorr classification system. Similar results were obtained in the finite element analysis in a previous study, and the reproducibility of the results was confirmed.²¹⁾ The trend remained the same regardless of the medullary cavity shape of the femur, stem type, or pre- and postoperative periods. This may be because of the appropriate stem size and intermediate alignment.

In this study, the von Mises stress and SED of the TL were larger than those of the Preserve. TL has a longer stem, and the distance from the loading point on the femoral head to the tip of the stem is longer than that of the Preserve. Consequently, the bending moment, which is the product of the load and moment arm, is expected to increase, leading to higher stress levels. Furthermore, the zone of the VOI of the TL is more distal than that of the Preserve; therefore, the effect of the TL VOI is more strongly affected. In the Dorr classification, the von Mises stress and SED were larger in both stems, except for Zones 1 and 7 of the reserve, in the following order: Dorr A < Dorr B < Dorr C. Generally, the wider the medullary cavity, the thinner the cortical bone.²²⁾ Thinner cortical bone tends to have a higher load per bone cross-sectional area and is more easily deformed, resulting in higher stress in Dorr C.

The rates of change in the von Mises stress and SED tended to be smaller in Zone 4 or Zone 5 and larger in Zone 1 or Zone 7 for both stems. This may be because the effect of stress shielding is stronger in the proximal region, and the values of the von Mises stress and SED are small; thus, a small change in the stress and SED results in a large rate of change. Excluding the results of Zone 1 in Dorr B using Preserve, the rates of change in the von Mises stress and SED tended to increase in the following order: Dorr C < Dorr B < Dorr A for both stems. When a

load was applied to the bone head, bending and compressive deformations occurred simultaneously. The insertion of a stiff stem increased the stiffness of the femur, resulting in smaller bending deformations and lower stress values, leading to stress shielding. Compressive deformation is not significantly affected by the stiffness of the stem but by the cross-sectional area of the bone. The thin cortical bone of the Dorr C-type has a smaller cross-sectional area than the others, and the stress tends to increase. Femurs with narrow medullary cavities have less bending and compressive deformations, even if a stem is inserted, resulting in a significant decrease in stress from the preoperative level. When the medullary cavity is wide, bending deformation is similarly small; however, compressive deformation has a greater effect, resulting in a greater stress reduction than in Dorr A.

In this study, Preserve exhibited a tendency for a smaller rate of change than TL; only Dorr C exhibited a tendency for a larger rate of change in the proximal femur, indicating that the effect of stress shielding is small for Dorr A and Dorr B owing to the use of short stems. The ideal stress distribution for the preoperative and postoperative stresses on the femur is an equal rate of change at each VOI. For Dorr A and Dorr B, the Preserve had a more natural stress distribution, similar to that of the preoperative femur. Preserve is a metaphyseal-diaphyseal fixation, and the cross-section of the stem is rectangular. Regarding Dorr C, as the medullary cavity from the femoral neck to the subtrochanter widens, Preserve increases the rate of change of von Mises stress and SED in the cross-section of the proximal femur because the size increase ratio of the stem is larger than that of the TL. The medullary cavity occupied by the stem is larger for Preserve. In other words, the "stiffness" effect associated with the volume fraction may be larger than that associated with the extension of stem length. In addition, the bone strength of the entire bone, including the trabecular bone in Dorr C, where the cortical bone is thin, becomes fragile. Therefore, the difference between the stiffness of Dorr C and that of the Dorr C stem is larger than that of other Dorr types, and the stress and SED of the Dorr C femur may be more influenced by the stiffness of Dorr C than by those of other Dorr types. Such an unbalanced rate of change in stress distribution in the femur significantly affects Dorr C, which has a thin cortical bone and is at risk of fracture.²³⁾ Therefore, in the finite element analysis, regarding the adaptation of both stems to the medullary cavity geometry, the stem with a large difference in the rate of change of von Mises stress and SED in each zone should have limited adaptation and the use of a short stem, especially for Dorr

C, is considered to increase the risk of fracture.

The limitations of this study are that it did not consider the difference in offset between the 2 stems, did not consider the stem contact area, was a stress analysis for walking only, did not consider the load during standing or stair climbing, is the result of a simulation in finite element analysis, and may not be an accurate *in vivo* mechanical evaluation depending on the zone. An accurate *in vivo* mechanical evaluation, depending on the zone, is not possible. Some zones had deviant values that could be considered outliers. As the offset increases, the bending moment increases, which may lead to an increase in stress. Initially, although a comparison using the same offset distance would have been appropriate, in this study, we decided to utilize the existing stem for the comparison in order to make it more realistic. Future studies should consider comparing stress distribution with existing offset types, particularly when standing and ascending or descending stairs. Additionally, only 1 case of short stem was actually used for Dorr C. This single case was compared to a tapered wedge and a short stem under the same condition, allowing for the understanding of the specificity and characteristics of this case through analysis, although only 1 case was used. However, there was certainly potential for selection bias. Though von Mises stress and SED increased in zone 1 of the Dorr B femur with the short stem, as shown in Table 5, this result could be due to minute differences in the contact conditions between the stem and femur, geometry errors in modeling, and calculation errors. Since the contact area of the stem varies depending on the shape of the femoral medullary cavity in detail, finite element analysis using a larger number of femur samples may provide a more accurate stress distribution, highlighting a critical aspect for future investigation.

In this study, we compared the distributions of von Mises stress and SED for Preserve and TL stems in relation to the luminal geometry of each Dorr classification. They revealed similar results, and the same trend was observed for the Dorr classification. However, the stresses were considered to increase in the TL because of the longer stem length and increase in the bending moment, which is the product of the load and moment arm. The rate of change was evaluated. For Dorr A and Dorr B, Preserve exhibited a more natural stress distribution similar to that of the pre-operative femur than TL. However, for Dorr C, the rate of change in von Mises stress and SED at the proximal femur was greater for Preserve than for TL. This suggests that the difference between TL and Preserve in terms of stem stiffness becomes larger and may cause greater effects, such as fracture in the early postoperative period, than other Dorr types. Therefore, caution may be warranted in the use of short stems, particularly when the femoral marrow cavity is wide. Further research is necessary to determine the ideal stem type for femurs with a wide medullary cavity.

CONFLICT OF INTEREST

No potential conflict of interest relevant to this article was reported.

ORCID

Tsuguaki Hosoyama

<https://orcid.org/0000-0002-8505-6534>

Nobuhiro Kaku <https://orcid.org/0000-0002-4041-1870>

Jonas A. Pramudita <https://orcid.org/0000-0002-5892-5925>

Yutaro Shibuta <https://orcid.org/0000-0001-5555-0905>

REFERENCES

1. Feyen H, Shimmin AJ. Is the length of the femoral component important in primary total hip replacement? *Bone Joint J.* 2014;96(4):442-8.
2. Drosos GI, Tottas S, Kougioumtzis I, Tilkeridis K, Chatzipapas C, Ververidis A. Total hip replacement using MINIMA® short stem: a short-term follow-up study. *World J Orthop.* 2020;11(4):232-42.
3. Sharkey PF, Albert TJ, Hume EL, Rothman RH. Initial stability of a collarless wedge-shaped prosthesis in the femoral canal. *Semin Arthroplasty.* 1990;1(1):87-90.
4. Khanuja HS, Vakil JJ, Goddard MS, Mont MA. Cementless femoral fixation in total hip arthroplasty. *J Bone Joint Surg Am.* 2011;93(5):500-9.
5. Glassman AH, Bobyn JD, Tanzer M. New femoral designs: do they influence stress shielding? *Clin Orthop Relat Res.* 2006;453:64-74.
6. Bozic KJ, Kamath AF, Ong K, et al. Comparative epidemiology of revision arthroplasty: failed THA poses greater clinical and economic burdens than failed TKA. *Clin Orthop Relat Res.* 2015;473(6):2131-8.
7. Toth K, Mecs L, Kellermann P. Early experience with the Depuy Proxima short stem in total hip arthroplasty. *Acta Orthop Belg.* 2010;76(5):613-8.

8. Blakeney WG, Lavigne M, Beaulieu Y, Puliero B, Vendittoli PA. Mid-term results of total hip arthroplasty using a novel uncemented short femoral stem with metaphyso-diaphyseal fixation. *Hip Int.* 2021;31(1):83-9.
9. Gilbert RE, Salehi-Bird S, Gallacher PD, Shaylor P. The Mayo Conservative Hip: experience from a district general hospital. *Hip Int.* 2009;19(3):211-4.
10. Cooper HJ, Jacob AP, Rodriguez JA. Distal fixation of proximally coated tapered stems may predispose to a failure of osseointegration. *J Arthroplasty.* 2011;26(6 Suppl):78-83.
11. Aro HT, Alm JJ, Moritz N, Makinen TJ, Lankinen P. Low BMD affects initial stability and delays stem osseointegration in cementless total hip arthroplasty in women: a 2-year RSA study of 39 patients. *Acta Orthop.* 2012;83(2):107-14.
12. Drosos GI, Touzopoulos P. Short stems in total hip replacement: evidence on primary stability according to the stem type. *Hip Int.* 2019;29(2):118-27.
13. Rodriguez-Buitrago A, Attum B, Cereijo C, Yusi K, Jahangir AA, Obremskey WT. Hemiarthroplasty for femoral neck fracture. *JBJS Essent Surg Tech.* 2019;9(2):e13.
14. Kwak DK, Bang SH, Lee SJ, Park JH, Yoo JH. Effect of stem position and length on bone-stem constructs after cementless hip arthroplasty. *Bone Joint Res.* 2021;10(4):250-8.
15. Bergmann G, Siraky J, Rohlmann A, Koelbel R. A comparison of hip joint forces in sheep, dog and man. *J Biomech.* 1984;17(12):907-21.
16. Lee PY, Lin KJ, Wei HW, et al. Biomechanical effect of different femoral neck blade position on the fixation of intertrochanteric fracture: a finite element analysis. *Biomed Tech (Berl).* 2016;61(3):331-6.
17. Heller MO, Bergmann G, Kassi JP, Claes L, Haas NP, Duda GN. Determination of muscle loading at the hip joint for use in pre-clinical testing. *J Biomech.* 2005;38(5):1155-63.
18. Gruen TA, McNeice GM, Amstutz HC. "Modes of failure" of cemented stem-type femoral components: a radiographic analysis of loosening. *Clin Orthop Relat Res.* 1979;(141):17-27.
19. Biemond JE, Aquarius R, Verdonschot N, Buma P. Frictional and bone ingrowth properties of engineered surface topographies produced by electron beam technology. *Arch Orthop Trauma Surg.* 2011;131(5):711-8.
20. Bergmann G, Deuretzbacher G, Heller M, et al. Hip contact forces and gait patterns from routine activities. *J Biomech.* 2001;34(7):859-71.
21. Kaku N, Pramudita JA, Yamamoto K, Hosoyama T, Tsumura H. Stress distributions of the short stem and the tapered wedge stem at different alignments: a finite element analysis study. *J Orthop Surg Res.* 2022;17(1):530.
22. Takeuchi S, Kageyama I, Awatake T, Kato S, Yamashita H. Enlargement of the femoral marrow cavity with aging. *Kai-bogaku Zasshi.* 1998;73(3):259-64.
23. Gromov K, Bersang A, Nielsen CS, Kallemose T, Husted H, Troelsen A. Risk factors for post-operative periprosthetic fractures following primary total hip arthroplasty with a proximally coated double-tapered cementless femoral component. *Bone Joint J.* 2017;99(4):451-7.